Polyelectrolyte association and solvation

Alexandros Chremos[1, a)] and Jack F. Douglas[1, b)]
Materials Science and Engineering Division, National Institute of Standards and Technology, Gaithersburg, MD, 20899, USA

(Dated: 10 July 2018)

There has been significant interest in the tendency of highly charged particles having the same charge to form dynamic clusters in solution, but an accepted theoretical framework that can account for this ubiquitous phenomenon has been slow to develop. The theoretical difficulties are especially great for flexible polyelectrolytes due to the additional complex coupling between the polyelectrolyte chain configurations and the spatial distribution of the ionic species in solution. For highly charged polyelectrolytes, this leads to the formation of a diffuse "polarizable" cloud of counter-ions around these polymers, an effect having significant implications for the function of proteins and other natural occurring polyelectrolytes, as emphasized long ago by Kirkwood and coworkers. To investigate this phenomenon, we perform molecular dynamics simulations of a minimal model of polyelectrolyte solutions that includes an explicit solvent and counter-ions, where the relative affinity of the counter-ions and the polymer for the solvent is tunable through the variation of the relative strength of the dispersion interactions of the polymer and ions. In particular, we find that these dispersion interactions can greatly influence the nature of the association between the polyelectrolyte chains under salt-free conditions. We calculate static and dynamic correlation functions to quantify the equilibrium structure and dynamics of these complex liquids. Based on our coarse-grained model of polyelectrolyte solutions, we identify conditions in which three distinct types polyelectrolyte association arise. We rationalize these types of polyelectrolyte association based on the impact of the selective solvent affinity on the charge distribution and polymer solvation in these solutions. Our findings demonstrate the essential role of the solvent in the description of the polyelectrolyte solutions, as well as providing a guideline for the development of a more predictive theory of the properties of the thermodynamic and transport properties of these complex fluids.

I. INTRODUCTION

Polyelectrolytes are of broad scientific and technological interest because they are crucial to biological function and are essential for the development of many modern materials and processes.[1] Polyelectrolyte solutions have been the focus of decades of theoretical and experimental investigations and observational patterns have been established, even though no generally accepted theory explaining these patterns currently exists.[2–12] In particular, small angle neutron scattering (SANS) studies show that these solutions normally exhibit two structural features in the angular dependence of the scattered intensity in the absence of salt: a primary peak, along with a steep upturn at very low scattering angles.[13–18] The absence of these scattering features in neutral polymers in solution[19] has triggered an ongoing theoretical discussion[20–23] regarding the origin of these structural features, and this has resulted in the development of numerous models aimed at describing these structural features. While considerable attention has been placed in understanding the scaling of the primary "polyelectrolyte peak" position with polymer concentration, no generally accepted model currently exists that can provide a microscopic description of all these structural features.

The steep upturn of the static structure at low angle in salt-free polyelectrolyte solutions has been interpreted as the formation of multi-chain domains.[17,22] Dynamic scattering studies[13,17,21] have revealed that these solutions exhibit a "fast mode" corresponding to the coupled interactions between the counter-ions and the polyelectrolyte, and a "slow mode" corresponding to the motion of the multi-chain domains. The formation of multi-chain domains by polyelectrolytes carrying the same charge evidently requires the existence of effective interchain attractions causing the chains to come into close proximity to each other. Several models have been proposed in the past that outline conditions at which attractive inter-chain attractions may rise.[23–25] However, most previous models of polyelectrolyte solutions treat the solvent as a structureless continuous medium that only indirectly influences the polyelectrolyte chains through the solvent's dielectric constant. However, an explicit solvent is required to model the competitive binding between the solvent and the counter-ions, along the polyelectrolyte backbone.

To highlight the significance of solvation in polyelectrolyte solutions, we first summarize the effects of solvation in the "simple" case of electrolyte solutions (with no polyelectrolyte chains). Electrolyte solutions having different salts exhibit a wide range of solution properties, such as the density, viscosity, and surface tension. Changes in these solution properties are typically discussed in terms of "chaotropic" and "kosmotropic" nature of the ions, corresponding to whether the ions decrease or increase the viscosity of the aqueous solu-

[a)] Electronic mail: alexandros.chremos@nist.gov
[b)] Electronic mail: jack.douglas@nist.gov

tion when the salt is added at low concentrations.[26–30] This phenomenon is linked phenomenologically to the Hoffmeister series[31] governing the solubility of the proteins in the same salts, but an understanding of how protein solubility in salt solutions and mobility changes upon adding salt to water without proteins is presently unclear. Observations by Collins,[32,33] and theoretical arguments by Ninham et al.,[34] suggest the importance of ion-size on the extent of ion-solvation and the dispersion interaction between ions and water, respectively, in understanding both the trends in the solution viscosity of aqueous solutions, and the origin of the Hofmeister series. Indeed, the ion solvation energy effectively reflects a combination of Coulombic and dispersion interaction contributions between the ions and the solvent molecules surrounding the ions.[35] Motivated by these general observations, we explored an explicit electrolyte solvent model in which the water-ion dispersion interaction parameter was determined by the ion solvation energy through the application of Born theory of ionic solvation to estimate the dispersion interaction strength.[36] We found that molecular dynamics simulations utilizing this model captured semi-quantitatively observed changes in solution viscosity and water diffusion coefficient on ion type,[36] an effect that classical coarse-grained pair-potential models had previously failed to reproduce.[37] Recent calculations of the same model reveal that several other thermodynamic properties, including the density, isothermal compressibility, and surface tension, can be understood via the solvent-ion interactions, suggesting that the chaotropic and kosmotropic effects primarily arise from ion solvation.[38] Thus, if the solvent interactions with the ionic species plays such a crucial role in modulating the electrolyte solution properties, then it is logical to expect analogous effects in polyelectrolyte solutions.

In our previous study,[39] we demonstrated that an enhanced affinity of the solvent for the counter-ions can influence the spatial distribution of the counter-ions associated with the polyelectrolyte chains, leading to ionization and localization of the counter-ions between the polyelectolytes. These ion-polymer correlations, in turn, result in the emergence of effective long-range interchain attractive interactions that induce chain clustering at low chain concentrations and the formation of voids (regions depleted of both counter-ions and polyelectrolyte chains, but occupied by solvent) at moderate polymer chain concentrations.[39] However, these findings are based on the variation of only one interaction parameter suggesting the potential of finding more intriguing structural behaviors of polyelectrolyte solutions. Indeed, we have investigated the effect of solvation in an isolated polyelectrolyte chain and we found that the solvation significantly influence the counter-ion distribution around the polyelectrolyte chains, as well as their conformational properties.[40,41]

In the present work, we investigate the effects of the solvent affinity for charged species and how it leads to heterogeneous structure formation in salt-free polyelectrolyte solutions. In particular, we use molecular dynamic simulations (MD) of a coarse-grained of polyelectrolyte solvent model[42–44] that includes an explicit solvent and counter-ions, along with energetic parameters that govern the relative affinity of the solvent for the counter-ions. This model accounts for the short-ranged interactions of solvent needed to address counter-ion and polymer solvation, while at the same time it enables long time and relatively large scales simulations that are required to study the associative behavior of polyelectrolyte solutions. In particular, we calculate the static structure factor $S(q)$ of the counter-ions and the polyelectrolyte chain segments for four different types of solvents, i.e., uncharged polymers in solution, no solvent affinity, solvent affinity for the counter-ions and solvent affinity for the polyelectrolyte segments. The location of the polyelectrolyte peak is quantified as a function of the polymer concentration and the strength of the solvent affinities. We also characterize the short-ranged interchain correlations by calculating the pair distribution function, $g(r)$. Finally, we calculate the intermediate scattering function and determine the relaxation times of the counter-ions and the polyelectrolyte segments. Overall, we find that the resulting heterogeneous structure formation arising from the type and strength of solvent affinity for the charged species changes in concert with the dynamics of polylectrolyte solutions.

Our paper is organized as follows. Section II contains details of the model and simulation methods. Results of the structure of the polyelectrolyte solution, as well as, the dynamics results at different solvent affinity for the charged species are presented in Section III. Section IV concludes the paper.

II. MODEL AND METHODS

We employ a bead-spring model of Lennard-Jones (LJ) segments bound by stiff harmonic bonds suspended in explicit LJ solvent particles, some of which are charged to represent counter-ions[42–44] All macro-ion segments, dissolved ions, and solvent particles are assigned the same mass m, size σ, strength of interaction ε. We set ε and σ as the units of energy and length; the cutoff distance for the LJ interaction potential is $r_c = 2.5\,\sigma$. The size and energy parameters between i and j particles are set as $\sigma_{ii} = \sigma_{jj} = \sigma_{ij} = \sigma$ and $\varepsilon_{ii} = \varepsilon_{jj} = \varepsilon_{ij} = \varepsilon$), except for two energy interaction parameters: the first interaction parameter is between the solvent particles and the positive ions ε_{cs} and the second interaction parameter is between the solvent particles and the polyelectrolyte segments ε_{ps}. Variation of the interaction energy parameters between different types of particles reflect the degree of chemical incompatibility between the polymer repeating units.[45] The primary focus of this study is on influence of ε_{cs} and ε_{ps} parameters on the structure and dynamics of salt-free polyelectrolyte solutions; a schematic of the various energetic parameters is presented in Fig. 1. All poly-

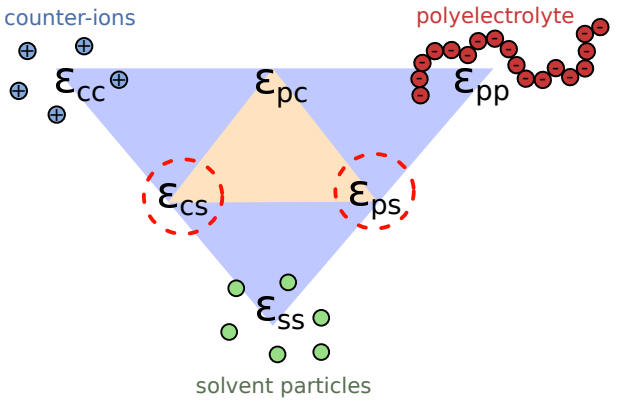

FIG. 1. Schematic illustrating the different energetic interactions between three species in polyelectrolyte solutions namely, the polyelectrolyte segments, the counter-ions, and the solvent. The parameters at the corners of the outer triangle correspond the self-interaction energy parameters and the parameters at the corners of the inner triangle correspond to the cross-energy interaction parameters.

electrolyte chains have a molecular mass of $M_w = 41$, carrying a $-e$ charge per segment, where e is the elementary charge, and the total polyelectrolyte charge is $Z_p = -M_w\, e$. The bonds between polymer segments are connected via a stiff harmonic spring, $V_H(r) = k(r-l_0)^2$, where $l_0 = \sigma$ is the equilibrium length of the spring, and $k = 1000\,\varepsilon/\sigma^2$ is the spring constant. All charged particles interact via the Coulomb potential (with a cut-off distance $10\,\sigma$) and a relatively short range Lennard-Jones potential of strength ε, and the particle-particle particle-mesh method is used.[46]

The system is composed of a total of $N = 256\,000$ particles in a periodic cube of side L and volume V. The system includes N_p polyelectrolyte chains and $N_+ = N_p|Z_p/e|$ counter-ions; the number of neutral particles is $N_0 = N - N_+ - N_p M_w$ and we define the charge fraction as $\varphi = (N_+ + N_p|Z_p/e|)/N$. All systems have neutral total charge. The Bjerrum length was set equal to $l_B = e^2/(\epsilon_s k_B T) = 2.4\,\sigma$, where T is the temperature, k_B is Boltzmann's constant, and ϵ_s is the dielectric constant of the medium. The systems were equilibrated at constant pressure and constant temperature conditions, i.e., reduced temperature $k_B T/\varepsilon = 0.75$ and reduced pressure $\langle P\rangle \approx 0.02$, and the production run were performed at constant temperature constant volume, maintained by a Nosé-Hoover thermostat. Typical simulations equilibrate for $4000\,\tau$ and data is accumulated over a $10\,000\,\tau$ interval, where $\tau = \sigma(m/\varepsilon)^{1/2}$ is the MD time unit; the time step used was $\Delta t\,/\,\tau = 0.005$.

III. RESULTS AND DISCUSSION

A. Structural properties of polyelectrolyte solutions

Polyelectrolytes release a significant fraction of their counter-ions into polar solvents into which they are dissolved and this ionization process results in long-range repulsive Coulomb interactions between the polymer segments that cause the polymer to swell. While many counter-ions associate with the chain backbone on a scale of the order of the chain segment size, many of the solvated counter-ions form a diffuse "cloud" around the chain due to residual unscreened polyelectrolyte charge. These distinct counter-ion bound states are transient with a constant dynamic exchange of counter-ions between them.[43,44,47] The spatial distribution of these weakly associated counter-ions and their effect on chain conformation make the modeling of polyelectrolytes challenging. Here, we explore how the variation of dispersion energy of the solvent with one of the ionic species influences the competitive binding between the counter-ions and the solvent particles with the polyelectrolyte backbone. We have explored the competitive binding for an isolated polyelectrolyte chain in solution in previous studies.[40]

Here, we investigate polyelectrolyte association for three types of solvents at the same electrostatic conditions, i.e., l_B and φ are fixed, unless stated otherwise. The first type of solvent is the "no selective solvent affinity" having $\varepsilon_{c,s}/\varepsilon = \varepsilon_{p,s}/\varepsilon = 1$, corresponding to a solvent having no preference for solvating either the counter-ions or the polyelectrolyte segments. For a no selective affinity solvent, the polyelectrolyte backbone is occupied by solvent particles and a fraction of counter-ions; counter-ions that are located at distances $r < 1.1\,\sigma$ from any polyelectrolyte segment are labeled as interfacial counter-ions.[44,48] As noted above, a significant fraction of counter-ions is located at longer distances, but is still associated with the polyelectrolyte chain, corresponding to the formation of a diffuse ionic cloud surrounding the polyelectrolyte chains. When the dispersion energies of the solvent for one of the ionic species start to become stronger then more interfacial counter-ions become dissolved in the solvent, as we have demonstrated in previous studies.[39–41] In other words, the solvent affinity for either the counter-ions or the polyelectrolyte segments leads to nearly complete ionization of the polymers. Thus, based on the relative solvent affinity for one of these ionic species, we label the solvent accordingly, i.e., "counter-ion affinity solvent" for solvents having $\varepsilon_{c,s}/\varepsilon > 1$ and $\varepsilon_{p,s}/\varepsilon = 1$, and "polyelectrolyte solvent affinity" $\varepsilon_{c,s}/\varepsilon = 1$ and $\varepsilon_{p,s}/\varepsilon > 1$. The choice of these parameters is to highlight the contribution of each dispersion interaction has on the structure and dynamic of the polyelectrolyte solution separately. The newly dissolved counter-ions continue to associate with the polyelectrolytes by enriching the surrounding counter-ion cloud, located at distances of $r/\sigma \approx 3$ to 5, see Figs. 2a and 2b. In other words, the affinity of the solvent on the charged species greatly influences the spatial distribution of counter-ions at the same the electrostatic conditions, e.g., same l_b and Debye screening length. Polyelectrolyte models based on an implicit solvent completely miss this basic phenomenon.

We now focus on understanding the structural nature

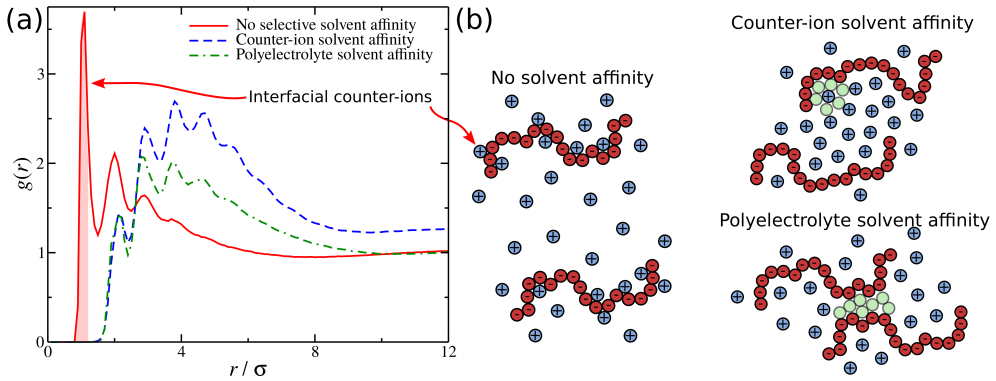

FIG. 2. (a) Pair correlation function between polyelectrolyte segments and counter-ions as a function of distance from the polyelectrolyte segments at different solvent affinities: no solvent affinity ($\varepsilon_{c,s}/\varepsilon = \varepsilon_{p,s}/\varepsilon = 1$); strong counter-ion solvent affinity ($\varepsilon_{c,s}/\varepsilon = 8$); strong polyelectrolyte solvent affinity ($\varepsilon_{p,s}/\varepsilon = 8$). The highlighted region corresponds to the interfacial counter-ions. The charge fraction for all cases was $\varphi = 0.032$. (b) Schematic illustrating the structure of different types of solvent affinities.

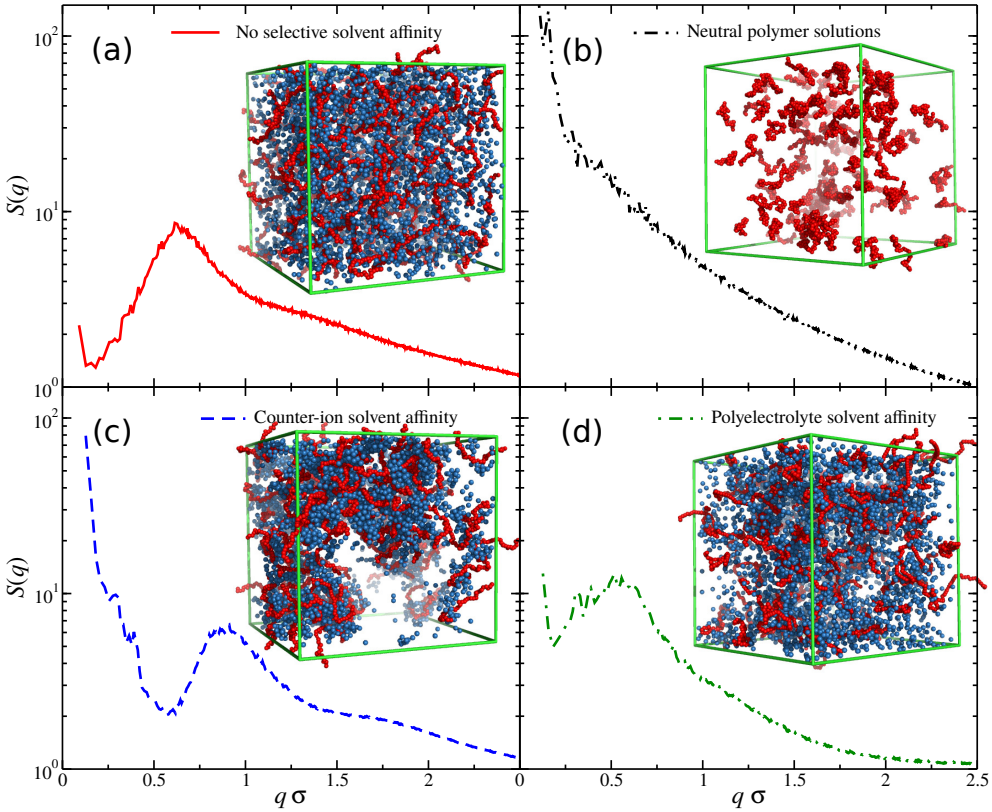

FIG. 3. Static structure factor $S(q)$ of polyelectrolyte segments for polyelectrolyte solutions having a charge fraction $\varphi = 0.032$ at different solvent affinities: (a) no solvent affinity ($\varepsilon_{c,s}/\varepsilon = \varepsilon_{p,s}/\varepsilon = 1$); (b) uncharged polymer solution; (c) strong counter-ion solvent affinity ($\varepsilon_{c,s}/\varepsilon = 8$); (d) strong polyelectrolyte solvent affinity ($\varepsilon_{p,s}/\varepsilon = 8$). Computer simulation screenshots of salt-free polyelectrolyte solutions for each case are presented; polyelectrolyte segments have red color, counter-ions have blue color, and the solvent is rendered invisible for clarity.

of polyelectrolytes in solutions based on our polyelectrolyte model, and we consider estimates in the average correlations in the positions of polyelectrolyte segments to quantify the different structures. In particular, we use the static structure factor $S(q)$, which is a suitable property for this purpose and describes the mean correlations in the positions of the polyelectrolytes. For a collection of point particles, $S(q)$ is defined as:

$$S(q) = \frac{1}{N_s} \left\langle \sum_{j=1}^{N_s} \sum_{k=1}^{N_s} \exp\left[-i\mathbf{q} \cdot (\mathbf{r}_j - \mathbf{r}_k)\right] \right\rangle, \quad (1)$$

where $i = \sqrt{-1}$, $q = |\mathbf{q}|$ is the wave number, $\mathbf{r}_j$ is the position of particle j, $\langle\rangle$ denote the time average, and N_s is the total number of polyelectrolyte segments defined as $N_s = N_{\rm p} M_{\rm w}$. Uncharged polymer chains in solution exhibit a monotonic decrease in $S(q)$, see Fig. 3b. For salt-free polyelectrolytes, $S(q)$ exhibits a primary peak located on a scale intermediate between the order of the polymer size and its location is influenced by the polymer concentration,[49,50] molecular architecture,[39] and charge valence.[17] Another characteristic feature of these complex liquids is the sharp upturn of the intensity of $S(q)$ at the low q-region, which varies with the particular system, and this scattering feature is often attributed to the chain clustering.[17,51,52] Qualitatively similar data is found for DNA, dendrimers, proteins, and other biological and synthetic polyelectrolytes.[18] We also note that the upturn at low q has been interpreted in the past as evidence of incipient macroscopic demixing promoted by hydrophobic interactions in aqueous solutions[53] or the presence of "dust" in the solution. However, the same behavior has been consistently observed from different groups for different solutions and polyelectrolytes,[13–18] including systems not having hydrophobic interactions,[16] suggesting that the upturn at low q reflects the formation of large scale structures.

In solvents having an absence of selective solvent affinity for the charged species, the polyelectrolyte becomes structured and a primary polyelectrolyte peak arises, as expected. We also find that in no selective affinity solvents, there is no or little low-angle enhancement of scattering intensity, see Fig 3a. Alternatively, if we treat the solvent as a continuum fluid in our polyelectrolyte model, as in the "standard restricted primitive model," then we find no steep upturn in the low q-region.[39] This suggests that when the interactions of the solvent for the charged species are relatively weak and balanced, i.e., in our model $\varepsilon_{\rm cs}/\varepsilon \approx \varepsilon_{\rm ps}/\varepsilon \lesssim 1$, then the polyelectrolyte chains tend to suppress the density fluctuations at long length scales by forming a homogeneous polyelectrolyte solution.

Enhancing the counter-ion solvation affinity results in a spatial re-arrangement of the counter-ions around the polyelectrolyte chain, as discussed above, but it also results in a shift in the location of the primary peak to larger q-values, meaning that the chains are closer together, and counter-ion solvation leads to a steep upturn in $S(q)$ at low q, see Fig 3c. As demonstrated in a previous study,[39] the affinity of the solvent for the counter-ions results in the emergence of effective long-range interchain attractive interactions that induce chain clustering at low chain concentrations (not reproduced here). Note that these long-range interchain interactions are mediated by the the structure of diffuse counter-ions surrounding the polyelectrolyte chains. In Fig. 4b, we present a comparison of the structure of counter-ions in a polyelectrolyte solution and in an electrolyte solution, where the solvent has strong affinity for the counter-ions; for more details on the electrolyte solution see Ref.[40]. It is evident from this comparison that the counter-ions with or without the polyelectrolyte chains exhibit sinusoidal-like behavior in $S(q)$, suggesting that when the solvent has strong affinity for the counterions, the counterions then form *random charge density waves*. Note that these random density waves are not well organized in space at a large length scale

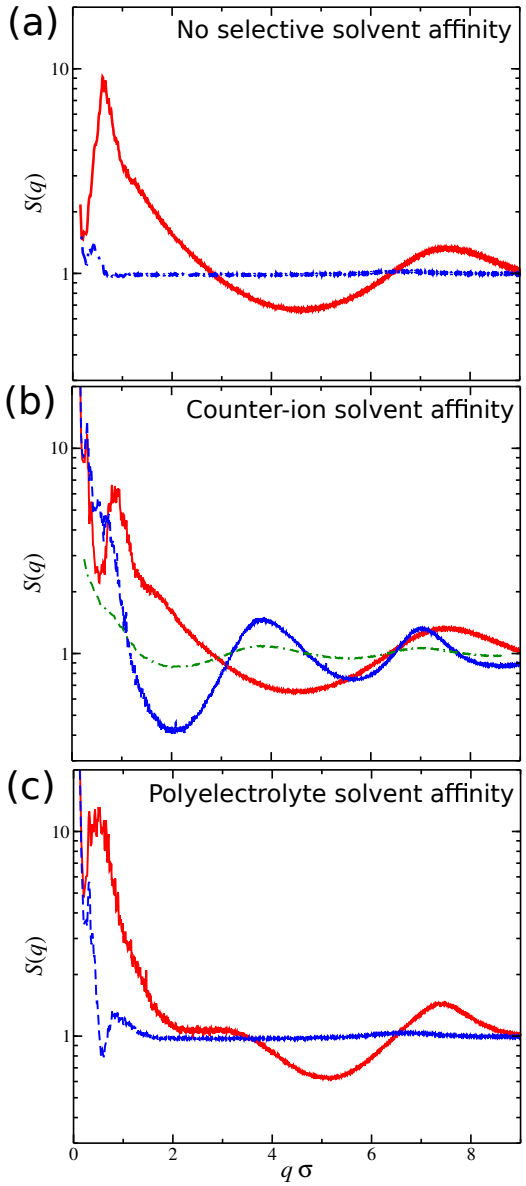

FIG. 4. Comparison of the structure factor $S(q)$ of the polyelectrolyte segments (red continuous line) and the counterions (blue dashed line) in a salt free polyelectrolyte solution at different solvent affinities: (a) no solvent affinity ($\varepsilon_{\rm c,s}/\varepsilon = \varepsilon_{\rm p,s}/\varepsilon = 1$); (b) strong counter-ion solvent affinity ($\varepsilon_{\rm c,s}/\varepsilon = 8$); (c) strong polyelectrolyte solvent affinity ($\varepsilon_{\rm p,s}/\varepsilon = 8$). The resulting $S(q)$ of the counter-ions in the case of electrolyte solutions is included as point of reference for the case of counter-ion solvent affinity (green dot-dashed line) as illustrated (b). The charge fraction for all cases was $\varphi = 0.032$.

and occur even in the absence of polyelectrolyte chains; these waves are an obvious source of correlations in the fluid giving rise to effective long-range attractions between the polymers mediated by the counter-ions. The clustering at low polymer concentrations results also to large regions of space in the solution significantly depleted of both polymers and counter-ions. In other words, large charge-free domains are formed, making the polyelectrolyte solution highly heterogeneous. At higher polymer concentrations, the clustering of the polyelectolyte chains leads to the formation of "voids" (bounded regions depleted by charges, but occupied by solvent), for more details about this phenomenon, see Ref. 39. Notably, the chain clustering and void formation are quite stable in time and exhibit characteristics of self-assembly rather than phase separation.[39]

Polyelectrolyte solvents having a high affinity for the polyelectrolyte segments result in the primary peak shifting to lower q-values with respect to the no selective affinity solvents, and a modest increase in $S(q)$ at lower q regions. This seems counter-intuitive because it suggests that there are density fluctuations at large length scales, while at the same time the average interchain distance is larger than in case of no selective affinity solvents. The physical picture that emerges from a visual inspection of the screenshots (Fig. 3) is that the polyelectrolyte chains form a network-like structure in this case. We quantify the short range correlations below, but here we note that the polyelectrolyte chains approach each other at much shorter distances then in the case of a solvent having high counter-ion affinity. Specifically, for high counter-ion affinity solvent the polymer chains approach each other on the order of the radius of gyration, while in the polyelectrolyte affinity solvent the polymer can be found at the order of a couple solvent particle diameters. While the polymers approach each other at such short distances, there is no physical contact or salt bridges, since the polymers are nearly fully solvated, see Fig. 2a. For the polymers to approach each other at such short distances, we do not observe the formation of large heterogeneous structures as we observed in the case of strong counter-ion solvation. For the screenshots in Figs. 3c and 3d, it is evident that the polyelectrolyte solvation leads to a relative homogeneous polyelectrolyte solvation, although a modest upturn in $S(q)$ is observed.

To better understand the effect of selective charge solvation, we keep track of the location of the polyelectrolyte peak ($q_{\rm peak}$) for a salt-free polyelectrolyte solution having $\varphi = 0.032$, and the results are presented in Fig. 5. For additional details on $S(q)$ for different polymer concentrations and at different solvent affinities, see supplementary information (SI). For modest enhancement of the solvation strength for either the counter-ion affinity or polyelectrolyte affinity (i.e., $\varepsilon_{\rm c,s}/\varepsilon \lesssim 4$ or $\varepsilon_{\rm p,s}/\varepsilon \lesssim 4$), the location of the polyelectrolyte peak remains at the same level as with no selective affinity solvents. However, there is significant shift in position for strong affinity solvents. Specifically, the ratio

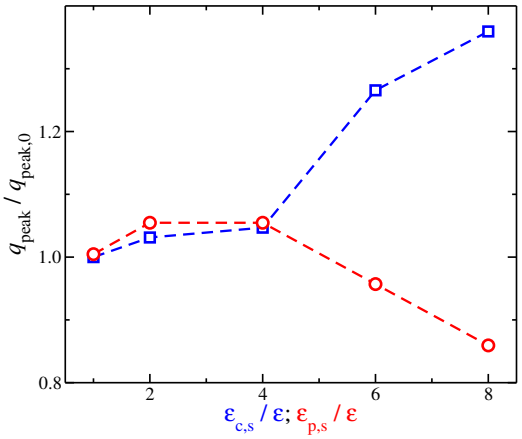

FIG. 5. Location of the polyelectrolyte peak position $q_{\rm peak}$ normalized by the peak location $q_{\rm peak,0}$ for no selective affinity solvent ($\varepsilon_{\rm c,s}/\varepsilon = \varepsilon_{\rm p,s} = 1$). The charge fraction for all cases was $\varphi = 0.032$. The symbols represent the counter-ion solvent affinity (squares) and the polyelectrolyte solvent affinity (circles).

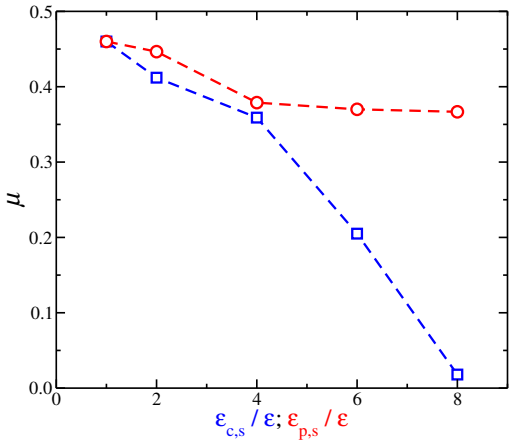

FIG. 6. Polyelectrolyte peak scaling exponent with polymer concentration $q_{\rm peak} \sim \rho_{\rm p}^{\mu}$ as a function of the strength of different solvent affinities. The symbols represent the counter-ion solvent affinity (squares) and the polyelectrolyte solvent affinity (circles). The charge fraction for all cases was $\varphi = 0.032$.

$q_{\rm peak}/q_{\rm peak,0}$ increases, meaning that the average distance between polyelectrolyte chains becomes smaller for strong counter-ion affinity solvents, $\varepsilon_{\rm c,s}/\varepsilon \gtrsim 4$.[39] On the other hand, the ratio $q_{\rm peak}/q_{\rm peak,0}$ increases for strong polyelectrolyte affinity solvents, $\varepsilon_{\rm p,s}/\varepsilon \gtrsim 4$. The deviation from unity is different between the two types of solvent affinity for the charged species illustrating the crucial role the solvent has in the structure formation of polyelectrolyte solvents.

The influence of the solvation for different charged species extents to scaling of "primary peak" position in $S(q)$ with polymer concentration, $\rho_{\rm p} = N_{\rm p}/V$. We briefly summarize what is known regarding the scaling of the primary peak. The peak broadens and shifts to

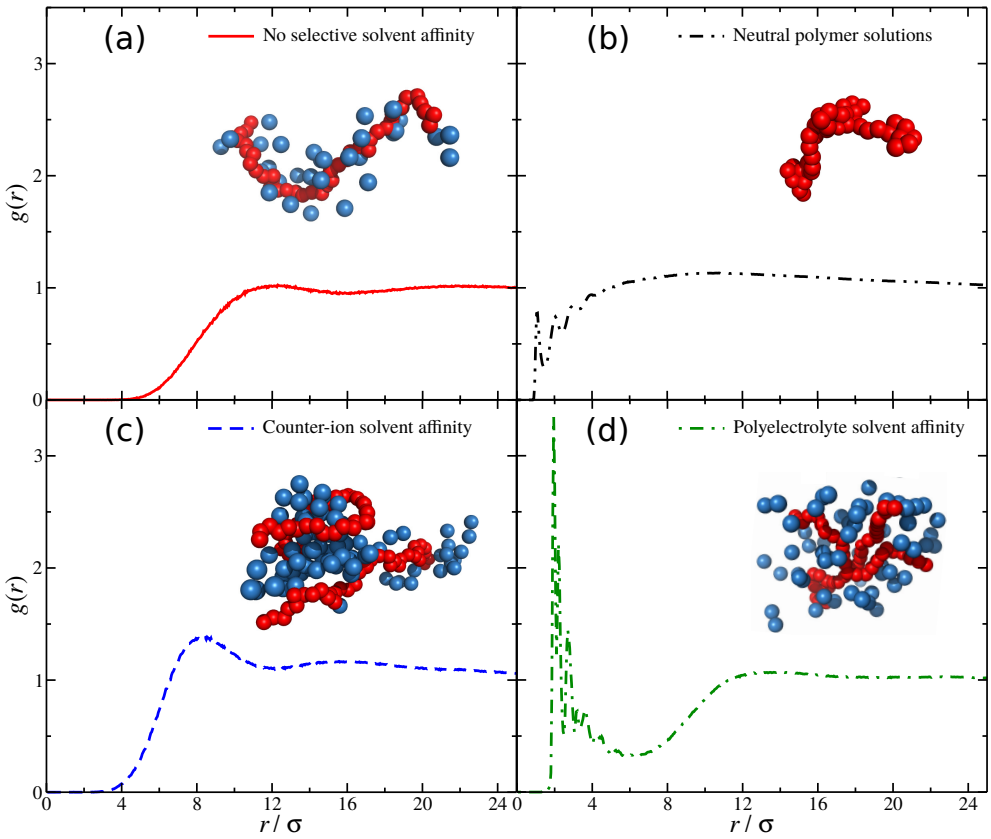

FIG. 7. Interchain segmental correlation function $g(r)$ for polyelectrolyte solutions having a charge fraction $\varphi = 0.032$ at different solvent affinities: (a) no solvent affinity ($\varepsilon_{c,s}/\varepsilon = \varepsilon_{p,s}/\varepsilon = 1$); (b) uncharged polymer solution; (c) strong counter-ion solvent affinity ($\varepsilon_{c,s}/\varepsilon = 8$); (d) strong polyelectrolyte solvent affinity ($\varepsilon_{p,s}/\varepsilon = 8$). Computer simulation screenshots of typical molecular conformations of a polylectrolyte chain in salt-free solutions for each case is presented, as well as the case of uncharged polymers; polyelectrolyte segments have red color, counter-ions have blue color, and the solvent is rendered invisible for clarity. We also note that the for (a) and (b) cases a single polymer chain is presented, while in the cases (c) and (d) a pair of associated polyelectrolyte chains are presented.

higher q-values as the concentration is increased, suggesting that this "liquid-like" local ordering progressively decreases with increasing concentration. There has been considerable theoretical effort to understand this variation in peak position, however, there is no agreed interpretation of this trend.[9,49,50,54] Most experiments for linear chain polyelectrolytes show that $q_{peak} \sim \rho_p^{\mu}$ scales with a power law exponent near $\mu \approx 1/3$ in dilute solutions and approximately $\mu \approx 1/2$ in semidilute solutions.[49,55] The exponent 1/3 represents the tendency of particles spatially localizing at interparticle distances. Since the particle concentration being proportional to their volume fraction, this behavior is typical in charged colloidal-like particles. Polyelectrolyte chains in dilute solution are often observed to follow this scaling behavior rather well, meaning that in dilute regime the polyelectrolyte chains can be effectively represented as point soft particles with long-ranged interactions. For semi-dilute polyelectrolyte chain solutions, scaling theories[56] predict $q_{peak} \sim \rho_{seg}^{1/2}$, which is consistent with simulation[57] and experimental studies.[49,58]

Our model calculations indicate that the scaling exponent μ can significantly vary between systems having different solvent affinities, as illustrated in Fig. 6. No solvent affinity results in $\mu \approx 0.46$ as we have shown in a previous study.[59] Solvent having counter-ion affinity greatly decreases the scaling exponent from $\mu \approx 0.46$ all the way to zero for $\varepsilon_{c,s}/\varepsilon = 8$. In the case of selective polyelectrolyte solvent affinity, we find a modest decrease of the scaling exponent. Based on the trends in Fig. 6, a scaling exponent 1/2 can be recovered by decreasing the strength of the solvent affinity ($\varepsilon_{c,s}$ or $\varepsilon_{p,s}$) to zero. In other words, the prediction of 1/2 is feasible in our model only when the solvent ceases to interact with the charged species.

Scaling arguments for polyelectrolyte solutions have predicted a concentration exponent of 1/2, but these arguments assume that polyelectrolyte solutions are *structurally homogeneous*. In contrast, many low angle neutron and x-ray scattering measurements on polyelectrolyte solutions indicate the presence of large excess scattering at low q, corresponding to some kind of large scale heterogeneity.[13–18] Moreover, the measured exponents, while often near 1/2, are observed to lie in a

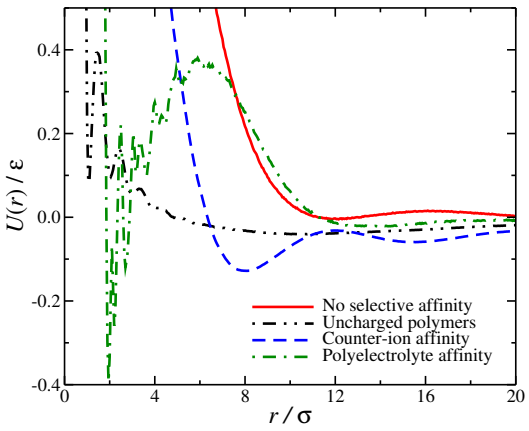

FIG. 8. Potential of mean force, $U(r) = -k_B T \ln[g(r)]$, based on the interchain segmental pair correlations, as a function of the distance. Results for different solvent affinities are also presented; the interaction parameters for each solvent affinity are the same as in Fig. 7. The charge fraction for all cases was $\varphi = 0.032$. The radius of gyration R_g of the polymer chain is approximately, $R_g/\sigma \approx 7$; see SI for details.

range between 1/3 and 1/2.[13–18] Our calculations indicate that the solvation of charged species can greatly influence the homogeneity of the polymer solution, as well as the concentration scaling exponent of the polyelectrolyte peak. The scaling of the polyelectrolyte peak position with polymer concentration would appear to be *non-universal*, depending on the many physical factors affecting the association of the polyelectrolytes in solution. This phenomenon obviously deserves further study from computational and experimental standpoints.

To better understand the trends observed in $S(q)$, we focus on the inter-segmental correlation function, $g(r)$, which is the Fourier transform of $S(q)$ and vice versa. The key advantage of $g(r)$ over $S(q)$ is that it captures the structural information at relative short length scales, while for longer length scales $S(q)$ becomes appropriate quantity. The $g(r)$ results for the different solvent affinities are presented in Fig. 7. No selective affinity solvents exhibit no conspicuous structural features. Specifically, the polyeletrolyte chains exhibit long range repulsions, evident from $g(r)$ becomes non-zero at relative long distances. Also, at long distances there are no pronounced peaks indicating that at these length scales the polymer chains fill the space as if the chains were particles in the vapor state. The effective interchain segmental interactions can also be seen by the calculation of the potential of mean force $U(r) = -k_B T \ln[g(r)]$. Indeed, for no selective affinity solvents $U(r)$ is purely repulsive as illustrated in Fig. 8. Uncharged polymers in solution can approach each other at much shorter distances to the point that occasionally the polymer can be in direct contact $r/\sigma \approx 1$. Uncharged polymers also exhibit long-range attractions, which originate from hydrodynamic forces acting through the solvent; the $U(r)$ for neutral polymers resulting in a small but wide minimum as illustrated in Fig. 8. Curiously, polymers in no selective affinity solvents do not exhibit these structural signatures in $g(r)$ for the long-range hydrodynamic attractions, suggesting other factors may contribute in the structure of the polyelectrolyte chains, e.g., the long-range Coulombic repulsions may suppress the structural signatures in $g(r)$. Counter-ion affinity solvents, as we discussed above, lead to the emergence of long-range attractions. This is evident in $g(r)$ with the emergence of a peak at length scales of the order of the radius of gyration.[39] These effective long-range attractions are due to the localization and clustering of counter-ions, which in turn bring closer together the polyelectrolyte chains, as seen in Fig. 7c.

We find for polyelectrolyte affinity solvents that there are effective short-range attractions and long-range repulsions. The short-ranged attractions is evident from the pronounced peak at distances $r/\sigma \approx 2$, which means that while the polyelectrolyte chains are fully ionized they can approach to each other at very short distances. This results to a $U(r)$ minimum located at $r/\sigma \approx 2$ as seen Fig. 8, while the minimum for counter-ion solvent affinity the minimum is located at $r/\sigma \approx 8$ which is closer to the size of the overall polymer chain. However, due to the electrostatic interactions between the chain segments only a fraction of the chains approach at such short distances, while the rest of the chains extends outward away from each other. This results in a long-range repulsion, which is evident in $g(r)$ at distances $3.5 < r/\sigma < 11$. The combination of short-range attractions and long-range repulsion effectively forms a branched polymer-like structure see the screenshot in Fig. 7d and from the schematic in Fig. 2b. At low concentrations, this short-range attraction is absent, but as the polymer concentration increases, pairs of polyelectrolyte chains form four-arm star-like structures and at higher polymer concentrations, these branched structures start to rebranch with each other by forming larger branched structures and evidently a percolating network.

We emphasize the significant variation in the structure of polyelectrolyte solutions, both at short and long length scales, as the ion-solvent affinity is varied. Contemporary mean field type theories do not take into the effects of solvation and as a result do not predict the emergence of structural heterogeneity in polyelectrolyte solutions. Based on our results on the structure of the polyelectrolyte solution becomes apparent that one cannot describe these solutions without an explicit solvent. To better understand the emergence of these structural features in polyelectrolyte solutions, we shift our focus on the dynamics of the charged species.

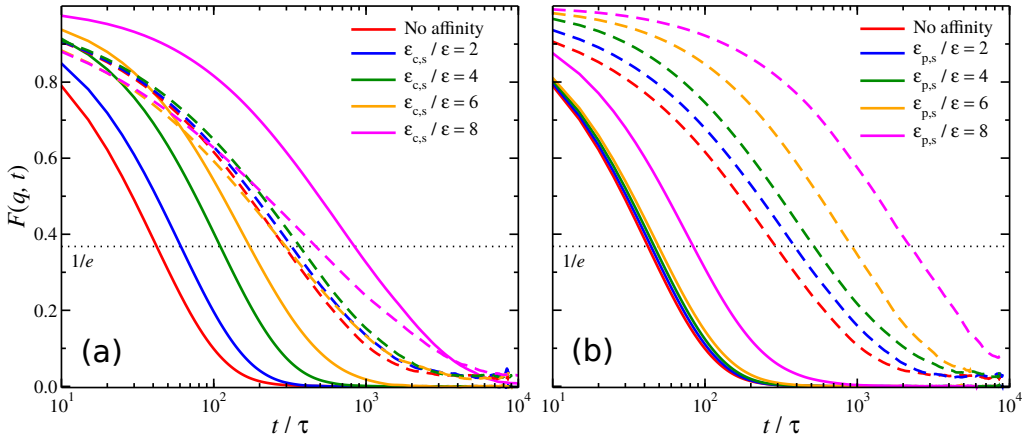

FIG. 9. Self-intermediate scattering function, $F(q,t)$, of counter-ions (continuous lines) and polyelectrolyte segments (dashed lines) in (a) counter-ion affinity solvents and (b) polyelectrolyte solvent affinity. The charge fraction for all cases was $\varphi = 0.032$.

B. Segmental and counter-ion dynamics of polyelectrolyte solutions

We briefly examine the dynamics of polyelectrolyte chains for different solvent affinities to gain insights on the origin heterogeneous structure formation in polyelectrolyte solutions. In particular, we probe the dynamics through the considerations of density fluctuations and the dynamical extension of the static structure factor, from which the structural relaxation time τ_α can be obtained. There is a large literature focusing on τ_α in the study of glass-forming liquids and we draw on this literature here.[60–63] Our analysis begins with how the solvent affinity influence the dynamics of the charged species, i.e., the polyelectrolyte chain segments and the counter-ions. To this end, we first calculate the self-intermediate scattering function:

$$F(q,t) = \frac{1}{N_{\rm p}M_{\rm w}} \left\langle \sum_{j=1}^{N_{\rm p}M_{\rm w}} \exp\left\{-i\mathbf{q}\cdot[\mathbf{r}_j(t) - \mathbf{r}_j(0)]\right\} \right\rangle, \tag{2}$$

where $\mathbf{r}_j(t)$ is the position of the polyelectrolyte segment or counter-ion j at the time t. The structural relaxation time τ_α may defined as $F(q = q_{\rm peak}, t = \tau_\alpha) = 1/e$, where e is the Euler's constant.

The resulting $F(q,t)$ curves for counter-ion affinity solvents are presented in Fig. 9. For no selective affinity solvent we find that $F(q,t)$ for counter-ions decays approximately six to seven time faster than the polyelectrolyte segments. This is to be expected, as in a real solution typically the counter-ions have higher mobility than the polyelectrolyte. However, as we increase the strength of the solvation of the counter-ions, we find that the $F(q,t)$ for the counter-ions decays slower while $F(q,t)$ for the polyelectrolyte segments remain approximately the same. For $\varepsilon_{\rm c,s}/\varepsilon = 8$ the mobility of the counter-ions becomes slower than the polyelectrolyte segments.

To better describe the changes rising from solvation of the charged species and highlight the difference between the counter-ion and polyelectrolyte solvent affinities, we consider the ratio of the structural relaxation of the polyelectrolyte segments over the structural relaxation of the counter-ions $\tau_{\alpha,s}/\tau_{\alpha,c}$ as a function of the strength of the solvent affinity. The trends for this ratio for the different types of solvent affinity and strengths is presented in Fig. 10; we note that the ratio is normalized by the value of $\tau_{\alpha,s}/\tau_{\alpha,c}$ for no selective affinity solvent ($\varepsilon_{\rm c,s}/\varepsilon = \varepsilon_{\rm p,s}/\varepsilon = 1$). An enhancement of the counter-ion solvent affinity resulting in a significant decrease of this ratio since for this type of solvent affinity the influence of the solvation impacts the mobility of the counter-ions. On the other hand, an enhancement of the polyelectrolyte solvent affinity results in a significant increase of $\tau_{\alpha,s}/\tau_{\alpha,c}$ because now the solvation inhibits the mobility of the polyelectrolyte segments. This is to be expected because essentially stronger solvation interactions with the polyelectrolyte chains leads to a tight solvation shell around the polyelectrolyte chain and thus the main way for the polyelectrolyte chain segments to relax is by carrying the solvation shell along them, which inhibits the segmental mobility.

The deviation from no solvent affinity solvents between different types solvent affinities runs parallel to the deviations observed in the primary polyelectrolyte peak, compare Figs. 5 and 10. This also reflects the close connection between structure and dynamics in polyelectrolyte solutions. From this comparison we can extract the following conclusion. For both ranges of solvent affinity, we observe that the solvated charged species starts to associate with molecules of its kind, leading to clustering and heterogeneous structure formation. In the case of counter-ion solvent affinity, we observe the formation of regions rich in counter-ions that are surrounded by polyelectrolyte chains. We obtain similar trends when the strength of the polyelectrolyte solvent affinity is varied, where the polyelectrolyte chains

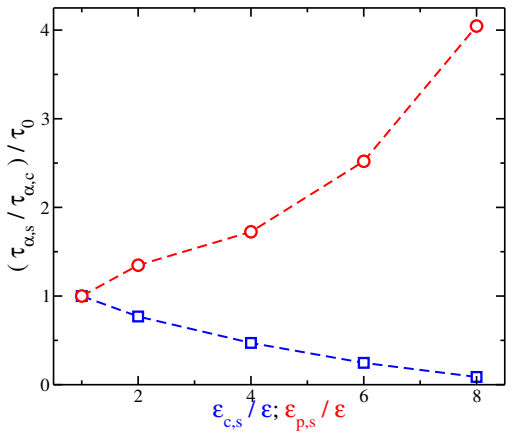

FIG. 10. Ratio of structural relaxation of polyelectrolyte segments over the structural relaxation of counter-ions, $\tau_{\alpha,s}/\tau_{\alpha,c}$, normalized by τ_0 which is the ratio $\tau_{\alpha,s}/\tau_{\alpha,c}$ for no selective affinity solvent ($\varepsilon_{c,s}/\varepsilon = \varepsilon_{p,s}/\varepsilon = 1$). The symbols represent the counter-ion solvent affinity (squares) and the polyelectrolyte solvent affinity (circles). The charge fraction for all cases was $\varphi = 0.032$.

closely associate with each other surrounded by a cloud diffuse fast-moving counter-ions. What is in common here is that the clustering occurs for the charged species having their mobility strongly inhibited by the effects of solvation. This effect appears to be similar to depletion effects observed colloidal solutions, where the uneven distribution of fast moving solvent particles around the colloids can lead to an effective attraction between these colloids.[64] A similar trend is found in polyelectrolyte solutions when we enhance significantly the solvent affinity for one the charged species. Overall, our current findings suggest that the heterogeneous structure formation in polyelectrolyte solutions is greatly influenced due to the solvation effects of the charged species. This is a new factor that must be considered in understanding of polyelectrolyte solutions and requires a general re-examination of the fundamental assumptions that underlie existing of polyelectrolyte and ion solution theories.

C. Emergent picture of polyelectrolyte solutions and prospects for coarse-grained modeling

Solvation evidently plays a crucial role in the structure formation in polyelectrolyte solutions since solvation dictates the ion distribution around the polyelectrolyte chain, which in turn impacts polyelectrolyte conformation and intermolecular interactions. The qualitative picture that emerges from our simulations is that the solvation of charged species causes ions to disassociate from the chain backbone, but the uncompensated charge of polymers and the ion and polymer solvation cause the counter-ions to become loosely localized within the domain pervaded by the polyelectrolyte segments.[44] This tendency of the polyelectrolytes to cluster is symptomatic of the asymmetry in the mobility of the counter-ions and polyelectrolyte segments. The extent of these solvation effects depends on the relative strength of the solvent affinity of the counter-ions and polyelectrolyte segments to the energy interaction parameter of the solvent molecules, so that polyelectrolyte structure formation is an outcome multiple competing interactions.

We consider a wider range of these interactions to determine the sensitivity of the solution structure to these interactions individually and to gain insight into the impact of the different dispersion interactions of the polyelectrolyte structures. In previous work,[36,38] we have shown how the dispersion interaction can be fixed for particular salts. Specifically, the dispersion energy interaction parameter between the solvent and counter-ions corresponds to ε_{cs} and for known monovalent ions the range of values start from 0.86 for Cs^+ to 1.6 for Li^+.[36,38] Even, larger values are expected for higher valent ions due to the higher charge density for a given ion size. The emphasis in the present paper is to understand qualitatively how the dispersion energy interaction between the solvent and charges influence the structure of salt-free polyelectrolyte solutions generally.

With regard to comparison of our polyelectrolyte and ionic model to experiment, we note that we have already rationalized a broad range of trends on the influence of specific salts on both dynamics, e.g., viscosity and solvent diffusion coefficient, and basic thermodynamic properties, such as density, surface tension, and isothermal compressibility, of aqueous salt solutions,[36,38] and the origin of "anomalous" low angle scattering,[17,59] in conjunction with the polyelectrolyte peak in monovalent salt-free polyelectrolyte solutions.[17,39] Our model also allowed us to understand the general experimental tendency of higher valent salts to enhance the flexibility of polyelectrolyte chains in solution[48] and the concomitant increase in the rate of relaxation of the solution layer around the polyelectrolyte chain.[65]

We also offer some thoughts about the prospects of implicit solvent modeling of polyelectrolyte solutions. Implicit solvent models have the advantage of being significantly faster than explicit solvent models, thus allowing the simulation of significantly larger systems compared to what is feasible with explicit solvent modeling. While the appeal of implicit solvent models of polyelectrolyte solutions is obvious, it is also important for the coarse-grained models to preserve the essential physics of these solutions. Our simulations suggest that solvation of charged species can profoundly influence the distribution of counter-ions around the polyelectrolyte chains so that any model that does not incorporate the effects of solvation can not provide a satisfactory description of these solutions. Even if a coarse-grained model is developed based on the potential of mean force description derived from an explicit solvent simulation, it is not clear that type of approach can treat the dynamics of polyelectrolyte solutions faithfully. Thus, the

development of implicit solvent model of polyelectrolyte solutions will require additional effort to ensure that the developed coarse-grained models capture the solvation effects described in the investigation.

IV. CONCLUSIONS

In summary, we investigated the associating behavior of salt-free polyelectrolyte solutions by utilizing molecular dynamic simulations of a coarse-grained model with an explicit solvent and counter-ions. The use of the explicit solvent allowed for the control of the degree of solvent affinity for the charged species. In particular, we find that an enhancement of the solvent interactions with one of the charged species leads to heterogeneous structure formation in the polyelectrolyte solution. Specifically, we consider a wide range of values of dispersion interactions of the counter-ions and the polyelectrolyte segments in comparison to those of the solvent and based on this analysis we identify three main behaviors of polyelectrolyte structure formation in salt-free solutions: (a) no selective solvent affinity results in repulsive interchain interactions leading in a homogeneous polyelectrolyte solution; (b) solvent affinity for the counter-ion leads to the emergence of long-range interchain attractive interactions due to the formation of disorganized charge density waves; (c) solvent affinity for the polyelectrolyte results in short-range interchain attractions and long-range repulsions leading to the formation of a gel-like network. The emergence of heterogeneous structure formation in the polyelectrolyte solutions influences the scaling of the polyelectrolyte peak in $S(q)$ as well as the relative location with respect to no selective affinity solvents. Finally, we calculated the intermediate scattering function and determined the structural relaxation of the polyelectrolyte segments and counter-ions. We find that the preferential solvent affinities greatly inhibit the mobility of the charged species depending on the type of solvent affinity. These results demonstrate that the dynamics and the heterogeneous structure formation in polyelectrolyte solutions are coupled, and highlight the direction in which future theories of polyelectrolyte solutions provide a direction for future theories.

Future work will focus on how polyelectrolyte alter the thermodynamic and transport properties of these complex fluids, the effects of added salt on rheological properties, e.g. time-salt superposition,[66] and the origin salt specific trends in polyelectrolyte miscibility as the Hofmeister series.[33,67] We expect our explicit solvent polyelectrolyte model to open a scientific window on a vast range of phenomena that is not conceivable within a solvent-free framework.

SUPPLEMENTARY MATERIAL

See supplementary material for information on polyelectrolyte peak in $S(q)$ as a function of polymer concentration and the radius of gyration results.

ACKNOWLEDGMENTS

We gratefully acknowledge the support of the NIST Director's Office through the NIST Fellows' postdoctoral grants program. Official contribution of the U.S. National Institute of Standards and Technology.

[1] M. Muthukumar, Macromolecules **50**, 9528 (2017).
[2] P. J. Flory, J. Chem. Phys. **21**, 162 (1953).
[3] G. S. Manning, J. Chem. Phys. **51**, 924 (1969).
[4] G. S. Manning, J. Chem. Phys. **51**, 3249 (1969).
[5] P. G. de Gennes, P. Pincus, and R. Velasco, J. Phys. (Paris) **37**, 1461 (1976).
[6] T. J. Odijk, J. Polym. Sci., Polym. Phys. Ed. **15**, 477 (1977).
[7] J. Skolnick and M. Fixman, Macromolecules **10**, 944 (1977).
[8] A. V. Dobrynin and M. Rubinstein, Prog. Polym. Sci. **30**, 1049 (2005).
[9] A. Yethiraj and C.-Y. Shew, Phys. Rev. Lett. **77**, 3937 (1996).
[10] A. Yethiraj, J. Chem. Phys. **108**, 11841192 (1998).
[11] G. Orkoulas, S. K. Kumar, and A. Z. Panagiotopoulos, Phys. Rev. Lett. **90**, 048303 (2003).
[12] M. Muthukumar, Polymer Science Series A **58**, 852 (2016).
[13] S. Föster, M. Schmidt, and M. Antonietti, Polymer **31**, 781 (1990).
[14] H. Matsuaka, D. Schwahn, and N. Ise, Macromolecules **24**, 4227 (1991).
[15] W. Essafi, F. Lafuma, and C. E. Williams, J. Phys. II **5**, 1269 (1995).
[16] B. D. Ermi and E. J. Amis, Macromolecules **30**, 6937 (1997).
[17] Y. Zhang, J. F. Douglas, B. D. Ermi, and E. J. Amis, J. Chem. Phys. **114**, 3299 (2001).
[18] F. Horkay and B. Hammouda, Colloid Polym. Sci. **286**, 611 (2008).
[19] P. J. Debye, Phys. Colloid Chem. **51**, 18 (1947).
[20] M. Sedlak and E. J. Amis, J. Chem. Phys. **96**, 817 (1992).
[21] M. Sedlak and E. J. Amis, J. Chem. Phys. **96**, 826 (1992).
[22] B. D. Ermi and E. J. Amis, Macromolecules **31**, 7378 (1998).
[23] M. Muthukumar, Proc. Natl. Acad. Sci. USA **113**, 12627 (2016).
[24] N. Grønbench-Jensen, R. J. Mashl, R. F. Bruinsma, and W. M. Gelbart, Phys. Rev. Lett. **78**, 2477 (1997).
[25] B. Ha and A. Liu, Phys. Rev. Lett. **79**, 1289 (1997).
[26] A. W. Omta, M. F. Kropman, S. Woutersen, and H. J. Bakker, Science **301**, 347 (2003).
[27] J. D. Batchelor, A. Olteanu, A. Tripathy, and G. J. Pielak, J. Am. Chem. Soc. **126**, 1958 (2004).
[28] Y. Marcus, Chem. Rev. **109**, 1346 (2009).
[29] Y. Marcus, Pure Appl. Chem. **82**, 1889 (2010).
[30] P. Ball and J. E. Hallsworth, Phys. Chem. Chem. Phys. **17**, 8297 (2015).
[31] F. Hofmeister, Arch. Exp. Pathol. Pharmacol. **24**, 247 (1888).
[32] K. D. Collins, Proc. Natl. Acad. Sci. U.S.A. **92**, 5553 (1995).
[33] K. D. Collins, G. W.Neilson, and J. E. Enderby, Biophys. Chem. **128**, 95 (2007).
[34] A. Salis and B. W. Ninham, Chem. Soc. Rev. **43**, 7358 (2014).
[35] T. T. Duignan, D. F. Parsons, and B. W. Ninham, Chem. Phys. Lett. **608**, 55 (2014).
[36] M. Andreev, A. Chremos, J. de Pablo, and J. F. Douglas, J. Phys. Chem. B **121**, 8195 (2017).
[37] J. S. Kim, Z. Wu, A. R. Morrow, A. Yethiraj, and A. Yethiraj, J. Phys. Chem. B **116**, 12007 (2012).

[38]M. Andreev, J. de Pablo, A. Chremos, and J. F. Douglas, J. Phys. Chem. B **122**, 4029 (2018).
[39]A. Chremos and J. F. Douglas, J. Chem. Phys. **147**, 241103 (2017).
[40]A. Chremos and J. F. Douglas, Gels **4**, 20 (2018).
[41]A. Chremos and J. F. Douglas, ACS Books (2018).
[42]R. Chang and A. Yethiraj, J. Chem. Phys. **118**, 6634 (2003).
[43]T. S. Lo, B. Khusid, and J. Koplik, Phys. Rev. Lett. **100**, 128301 (2008).
[44]A. Chremos and J. F. Douglas, Soft Matter **12**, 2932 (2016).
[45]A. Chremos, A. Nikoubashman, and A. Z. Panagiotopoulos, J. Chem. Phys. **140**, 054909 (2014).
[46]R. W. Hockney and J. W. Eastwood, *Computer Simulation Using Particles* (Taylor and Francis, New York, 1989).
[47]D. Hinderberger, G. Jeschke, and H. W. Spiess, Macromolecules **355**, 9698 (2002).
[48]A. Chremos and J. F. Douglas, J. Chem. Phys. **144**, 164904 (2016).
[49]L. Wang and V. A. Bloomfield, Macromolecules **24**, 5791 (1991).
[50]A. Yethiraj, Phys. Rev. Lett. **78**, 3789 (1997).
[51]H. Matsuoka, D. Schwahn, and N. Ise, Macromolecules **24**, 4227 (1991).
[52]F. Boué, J. P. Cotton, and G. Jannick, J. Chem. Phys. **101**, 2562 (1994).
[53]M. Shibayama and T. Tanaka, J. Chem. Phys. **102**, 9392 (1995).
[54]E. E. Maier, R. Krause, M. Deggelmann, M. Hagenbuchle, and R. Weber, Macromolecules **25**, 1125 (1992).
[55]E. E. Maier, S. F. Schulz, and R. Weber, Macromolecules **90**, 7 (1989).
[56]P. G. de Gennes, P. Pincus, F. Brochard, and R. M. Velasco, J. Phys. (Paris) **37**, 1461 (1976).
[57]M. J. Stevens and K. Kremer, J. Chem. Phys. **103**, 1669 (1995).
[58]V. M. Prabhu, M. Muthukumar, G. D. Wignall, and Y. B. Melnichenko, J. Chem. Phys. **119**, 4085 (2003).
[59]A. Chremos and J. F. Douglas, J. Chem. Phys. **147**, 044906 (2017).
[60]P. G. Debenedetti and F. H. Stillinger, Nature **410**, 259 (2001).
[61]F. W. Starr and J. F. Douglas, Phys. Rev. Lett. **106**, 115702 (2011).
[62]B. A. Pazmino Betancourt, J. F. Douglas, and F. W. Starr, Soft Matter **9**, 241 (2013).
[63]A. Chremos and J. F. Douglas, J. Chem. Phys. **143**, 111104 (2015).
[64]H. N. Lekkerkerker and R. Tuinier, *Colloids and the depletion interaction* (Springer, 2011).
[65]J. H. Roh, M. Tyagi, R. M. Briber, S. A. Woodson, and A. P. Sokolov, J. Am. Chem. Soc. **133**, 16406 (2011).
[66]E. Spruijt, J. Sprakel, M. Lemmers, M. A. Cohen Stuart, and J. van der Gucht, Phys. Rev. Lett. **105**, 208301 (2010).
[67]M. G. Cacace, E. M. Landau, and J. J. Ramsden, Quarterly Reviews of Biophysics **30**, 241 (1997).

Supplementary Information: Polyelectrolyte association and solvation

Alexandros Chremos[1, a)] and Jack F. Douglas[1, b)]
Materials Science and Engineering Division, National Institute of Standards and Technology, Gaithersburg, MD, 20899, USA

I. RADIUS OF GYRATION

The size of the polyelectrolyte chains can be described by the radius of gyration, R_g. We find a modest increase of R_g with increasing the solvent affinity for the charged species, either with an increase in the strength of the dispersion interaction between the solvent and the counter-ions, $\varepsilon_{c,s}$ or with the strength of the dispersion interaction between the solvent and the polyelectrolyte segments, $\varepsilon_{p,s}$, see Fig. S1. This is due the ionizstion of the backbone chain leading to stronger repulsions between the polyelectrolyte segments and thus swelling further the polyelectrolyte chain. However, for strong solvent affinities (for either $\varepsilon_{c,s}/\varepsilon \gtrsim 3$ or $\varepsilon_{p,s}/\varepsilon \gtrsim 3$) we find that the chain size starts to decrease. In previous work,[1] we have examined the polymer size of an isolated polyelectrolyte chain in an electrolyte solution and we found similar trends. There is one notable difference, however, while in our current study we find that the solvent affinity for the polyelectrolyte segments results in an overall $R_g(\varepsilon_{p,s}) \gtrsim R_g(\varepsilon_{c,s})$, but in the case of an isolated polyelectrolyte chain in solution, the R_g of the chain becomes smaller when there is strong solvent affinity for the polyelectrolyte segments than a strong solvent affinity for the counter-ion.[1]

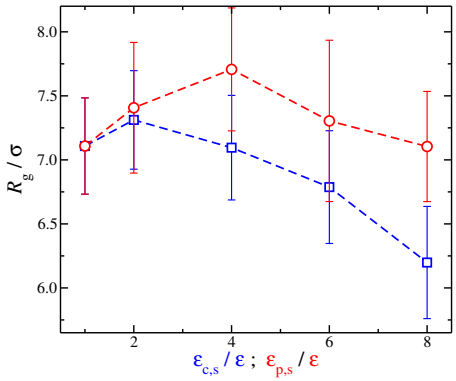

FIG. S1. Average radius of gyration, R_g, of polyelectrolyte chains in a solution having charge fraction $\varphi = 0.032$ as a function of the solvent affinity for the counter-ions, $\varepsilon_{c,s}$ (squares), and the solvent affinity for the polyelectrolyte segments $\varepsilon_{p,s}$ (circles). The error-bars correspond to one standard deviation.

II. STATIC STRUCTURE FACTOR

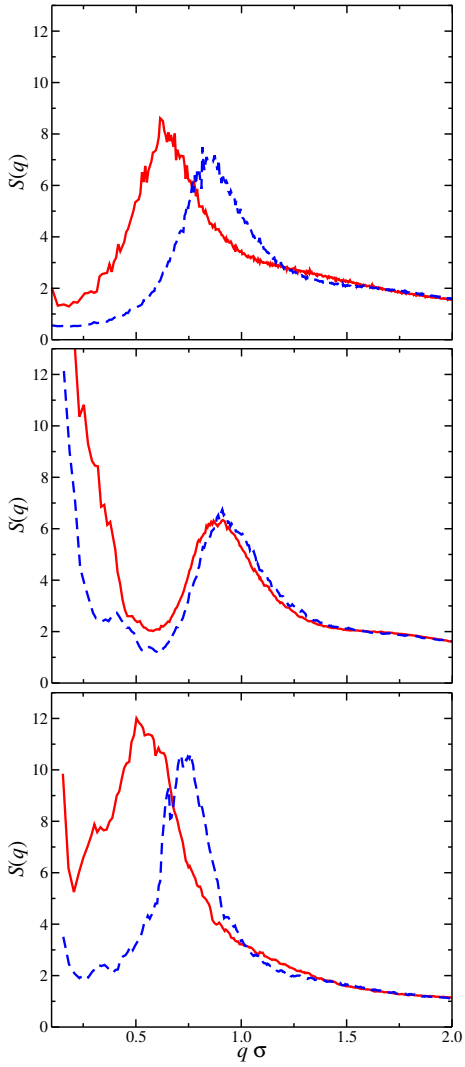

FIG. S2. Structure factor of polyelectrolyte solutions at different polymer concentration having charge fraction $\varphi = 0.032$ (red continuous line) and $\varphi = 0.064$ (blue dashed line) and at different solvent affinities: (a) No selective affinity, (b) counter-ion selective solvent affinity $\varepsilon_{c,s}/\varepsilon = 8$, and (c) polyelectrolyte selective solvent affinity $\varepsilon_{p,s}/\varepsilon = 8$.

The static structure factor, $S(q)$, is a suitable property for probing the structural nature of polyelectrolytes in solutions based on our polyelectrolyte model. This quantity describes the mean correlation in the positions of the polyelectrolyte segments. For a collection of point

[a)] Electronic mail: alexandros.chremos@nist.gov
[b)] Electronic mail: jack.douglas@nist.gov

particles, $S(q)$ is defined as:

$$S(q) = \frac{1}{N_s} \left\langle \sum_{j=1}^{N_s} \sum_{k=1}^{N_s} \exp\left[-i\mathbf{q}\cdot(\mathbf{r}_j - \mathbf{r}_k)\right] \right\rangle, \quad (1)$$

where $i = \sqrt{-1}$, $q = |\mathbf{q}|$ is the wave number, $\mathbf{r}_j$ is the position of particle j, $\langle\rangle$ denote the time average, and N_s is the total number of polyelectrolyte segments defined as $N_s = N_\mathrm{p} M_\mathrm{w}$.

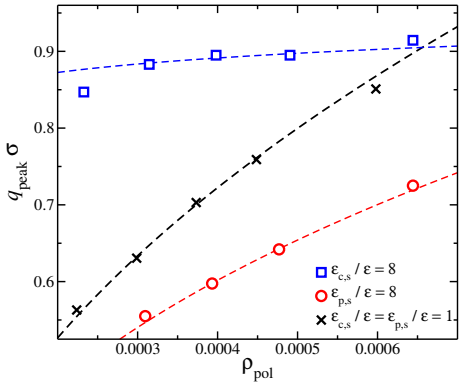

FIG. S3. Location of the peak location q_peak in the structure factor of the polyelectrolyte chains in solution as function of the polymer concentration, $\rho_\mathrm{pol} = N_\mathrm{p}/V$ at three different solvation affinities. The dashed lines are fits over the range $0.0003 < \rho_\mathrm{pol} < 0.0006$ based on the power-law relation, $q_\mathrm{peak} \sim \rho_\mathrm{peak}^{\nu}$.

Typical results of $S(q)$ for polyelectrolyte chain in solution at different polymer concentrations and at different solvent affinities are presented in Fig. S2. It is evident from the results that the solvation influences the excess scattering at low q at different polymer concentrations, $\rho_\mathrm{pol} = N_\mathrm{p}/V$. We discuss these trends in main manuscript and for the case of counter-ion solvation in Ref. 2. Solvation also influences the peak location in $S(q)$ and the rate at which the peak is shifted by adding polymers into the solution. Previously, we studied[3] trends in q_peak for a no selective affinity solvent ($\varepsilon_\mathrm{c,s}/\varepsilon = \varepsilon_\mathrm{p,s}/\varepsilon = 1$) and found that q_peak scales with ρ_pol as, $q_\mathrm{peak} \sim \rho_\mathrm{pol}^{\nu}$, where ν is scaling exponent $\nu \approx 0.46$.

We track the location of the polyelectrolyte peak in $S(q)$ for different polymer concentrations and solvent affinities. Typical results for q_peak trends as a function of ρ_pol at different solvent affinities are presented in Fig. S3. For strong affinity solvents for the counter-ions ($\varepsilon_\mathrm{c,s}/\varepsilon = 8$) results in high values of q_peak, but they have little variation with ρ_pol, resulting to relatively small scaling exponent ν. For strong affinity solvents for the polyelectrolyte segments ($\varepsilon_\mathrm{p,s}/\varepsilon = 8$) result in low values of q_peak and having a modest variation with ρ_pol. For a no selective affinity solvent ($\varepsilon_\mathrm{c,s}/\varepsilon = \varepsilon_\mathrm{p,s}/\varepsilon = 1$), $S(q)$ exhibits q_peak values that lay in between the solvent affinity for the counter-ions and the polyelectrolyte segments. For each type of solvent affinity, we fit the q_peak values of different solvent affinities to $q_\mathrm{peak} \sim \rho_\mathrm{pol}^{\nu}$ to determine ν. We note that the fitting was performed in the range of polymer concentrations $0.0003 < \rho_\mathrm{pol} < 0.0006$. We discuss the trends in the scaling exponents in the main manuscript.

[1] A. Chremos and J. F. Douglas, Gels **4**, 20 (2018).
[2] A. Chremos and J. F. Douglas, J. Chem. Phys. **147**, 044906 (2017).
[3] A. Chremos and J. F. Douglas, J. Chem. Phys. **147**, 241103 (2017).